Available online at www.sciencedirect.com
ScienceDirect
Biochemical and Biophysical Research Communications 369 (2008) 240–246
BBRC
www.elsevier.com/locate/ybbrc

Biophysical characterization of the EF-hand and SAM domain containing Ca^{2+} sensory region of STIM1 and STIM2

Le Zheng, Peter B. Stathopulos, Guang-Yao Li, Mitsuhiko Ikura *

Division of Signaling Biology, Ontario Cancer Institute and Department of Medical Biophysics, University of Toronto, Toronto, Ont., Canada M5G 1L7

Received 28 September 2007
Available online 31 December 2007

Abstract

Stromal interaction molecule 1 (STIM1) is an endoplasmic reticulum (ER)-membrane associated Ca^{2+} sensor which activates store-operated Ca^{2+} entry (SOCE). The homologue, STIM2 possesses a high sequence identity to STIM1 (~61%), while its role in SOCE seems to be distinct from that of STIM1. In order to understand the underlying mechanism for the functional differences between STIM1 and STIM2, we investigated the biophysical properties of the luminal Ca^{2+}-binding region which contains an EF-hand motif and a sterile α-motif (SAM) domain (hereafter called EF–SAM; residues 58–201 in STIM1 and 149–292 in STIM2). STIM2 EF–SAM has a low apparent Ca^{2+}-binding affinity (K_d ~0.5 mM), which is similar to that reported for STIM1 EF–SAM. In the presence of Ca^{2+}, STIM2 EF–SAM is monomeric and well-folded, analogous to what was previously observed for STIM1 EF–SAM. In contrast to apo STIM1 EF–SAM, apo STIM2 EF–SAM is more structurally stable and does not readily aggregate. Our circular dichroism (CD) data demonstrate the existence of a long-lived, well-folded monomeric state for apo STIM2 EF–SAM, together with a less α-helical/partially unfolded aggregated state which is detectable only at higher protein concentrations and higher temperatures. Our biophysical studies reveal a structural stability difference in the EF–SAM region between STIM1 and STIM2, which may account for their different biological functions.

Keywords: STIM1; STIM2; EF–SAM; Store-operated calcium entry; Aggregation; CD; NMR; Orai; CRAC

Cytoplasmic Ca^{2+} concentration is tightly regulated by various pathways [1,2]. Inositol triphosphate (IP_3)-mediated stimulation of Ca^{2+} release from the ER plays a vital role in calcium homeostasis in the cell [3]. The resulting store depletion further leads to a magnification of Ca^{2+} entry through a mechanism known as the store-operated Ca^{2+} entry (SOCE), which is a major Ca^{2+} entry pathway in electrochemically non-excitable cells [4–7]. This cellular mechanism is known to be the key to regulating long-term cellular processes such as gene transcription, cell growth and cell division and refilling intracellular stores [1]. Although the concept was proposed more than twenty years ago, the molecular makeup and the coupling mechanism between the ER stores and the plasma membrane (PM) Ca^{2+} channels had been largely undefined until recently.

In 2005, by using interfering and small RNA screens, two groups independently revealed that STIM1 is essential for store-operated Ca^{2+} (SOC) influx [8,9]. Subsequent studies supported a role for STIM1 as the long sought-after Ca^{2+} sensor which detects the fall of Ca^{2+} concentration in the ER lumen and as the transducer that conveys the ER Ca^{2+}-depletion signal to the SOC channels on the PM [10–12]. After the IP_3-mediated Ca^{2+} release from the ER, the reduced Ca^{2+} concentration triggers STIM1 molecules on the ER membrane to accumulate and redistribute into puncate close to ER–PM junctions which then activate Ca^{2+} release–activated Ca^{2+} (CRAC) channels and SOC influx.

* Corresponding author. Address: MaRS Toronto Medical Discovery Tower, Room 4-804, 101 College Street, Toronto, Ont., Canada M5G 1L7. Fax: +1 416 581 7564.
E-mail address: mikura@uhnres.utoronto.ca (M. Ikura).

0006-291X/$ - see front matter © 2007 Elsevier Inc. All rights reserved.
doi:10.1016/j.bbrc.2007.12.129

STIM1 is a type I transmembrane protein containing 685 amino acids and is mainly localized on the ER membrane (~75%) with the remaining on the PM (~25%). The N-terminus is in the ER lumen or extracellular space and contains a single canonical EF-hand Ca^{2+}-binding motif and a SAM domain, a well-known protein–protein interaction module. The C-terminus is in the cytoplasm and consists of two coiled-coil domains, a Pro/Ser-rich region, and a Lys-rich region (Fig. 1) [13–16].

In vertebrates, STIM1 has a closely related homologue, STIM2. STIM2 is also a type I transmembrane protein and contains 833 amino acids but is only found on the ER. The two molecules share similar domain architecture (Fig. 1), with the N-terminal EF-hand and SAM domains in the ER lumen and the C-terminal domains in the cytoplasm. However, the cellular behavior of the two and the role of STIM2 in SOCE is still unclear. Liou et al. [8] reported that knockdown of STIM2 abrogates SOCE, whereas Roos et al. [9] showed a similar treatment has no such effect. Overexpression of STIM2 inhibits STIM1-mediated SOCE activation [17]. When STIM2 is co-overexpressed with the store-operated channel protein Orai1, it constitutively (Ca^{2+}-independently) activates SOCE [18]. A recent study, however, demonstrates that STIM2/Orai1 overexpression regulates SOCE channels in both store-dependent and -independent manners [30]. Nevertheless, the ability of STIM2 to increase SOCE implies that under certain conditions, STIM2 might mimic STIM1 and play a role in regulating SOCE pathway. Lack of detailed biochemical and biophysical understanding of both STIM1 and STIM2 hinders the full appreciation of these homologues in the mechanism underlying SOCE.

Our previous studies showed that recombinant STIM1 EF–SAM binds to Ca^{2+} with a low affinity (K_d ~0.2–0.6 mM) and aggregates only in the absence of Ca^{2+}, analogous to the cellular observation of Ca^{2+}-depletion dependent punctae formation of STIM1 [19]. In the present report we have studied both STIM1 and STIM2 EF–SAM by means of CD spectroscopy, nuclear magnetic resonance (NMR) spectroscopy, and other biophysical techniques. Our data show that STIM2 has distinct structural properties from STIM1, which may be important in the regulatory role of STIM2 in SOCE.

Materials and methods

Protein expression and purification. Human STIM1 and STIM2 cDNAs were from Origene Technologies, Inc. The coding region of STIM1 EF–SAM (residue 58–201) or STIM2 EF–SAM (residue 149–292) was subcloned into pET28a vector (Novagen, Inc.) using NheI and XhoI restriction enzyme sites. All recombinant protein expression and purification was performed as previously described [19]. Protein concentration was measured using $\varepsilon_{280nm} = 1.40\ (mg\ ml^{-1})^{-1}\ cm^{-1}$. All experiments were performed in 20 mM Tris–HCl pH 7.5, 100 mM NaCl, with 5 mM $CaCl_2$ for Ca^{2+}-loaded (holo) samples or 1 mM EDTA for Ca^{2+}-free (apo) samples.

CD spectroscopy. Far-UV CD spectra were recorded on a Jasco J-815 CD spectrometer. Data were collected in 1-nm increments using a 0.01 cm-path length cell, 8-s averaging time and 1-nm bandwidth. Spectra were corrected for buffer contributions. Thermal melts were acquired at a scan rate of 1 °C min^{-1}.

NMR Spectroscopy. NMR experiments were performed on 800 MHz AVANCE II (Bruker, Inc.) or 600 MHz Unity/Innova NMR spectrometers (Varian, Inc.) equipped with cryogenic, triple resonance probes. ^{1}H–^{15}N heteronuclear single quantum coherence (HSQC) spectra were recorded with 2048 (^{1}H) × 256 (^{15}N) points and 16 scans per increment.

SEC and light scattering. Size exclusion chromatography (SEC) was performed on a Superdex 200 10/300 GL column (GE Healthcare). Multi-angle light scattering (MALS) measurements were performed in-line using the three-angle (45, 90, 135°) miniDawn static light-scattering instrument with a 690-nm laser (Wyatt Technologies, Inc.). Molecular weight was calculated using ASTRA software (Wyatt Technologies, Inc.) based on Zimm plot analysis using a refractive index increment, $dn\,dc^{-1} = 0.185\ l\ g^{-1}$.

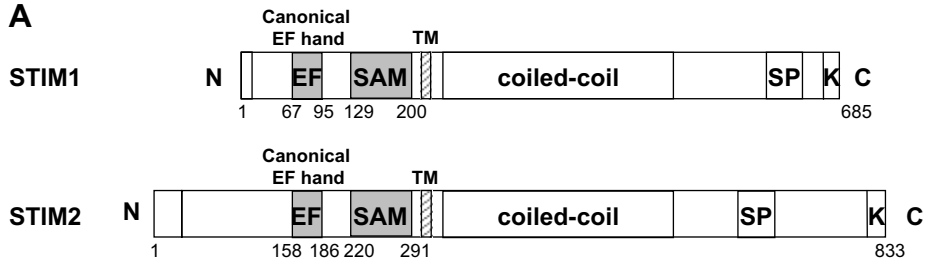

Fig. 1. Structural analysis of STIM proteins. (A) Schematic presentation of human STIM1 and STIM2 domains. (B) Sequence alignment of the EF–SAM region of STIM proteins from *homo sapiens* (h); *Mus musculus* (m); *Xenopus laevis* (x); *Drosophila melanogaster* (d) and *Caenorhabditis elegans* (c). X, Y, Z, −y, −x, and −z represent the first, second, third, fourth, fifth, and sixth Ca^{2+} ligand.

Results

STIM1 and STIM2 EF–SAM have similar Ca^{2+}-binding affinities

Our previous study indicated that STIM1 EF–SAM binds Ca^{2+} with an apparent dissociation constant, K_d of ~0.2–0.6 mM [19]. Obtaining an accurate K_d for STIM2 EF–SAM proved difficult using $^{45}Ca^{2+}$, intrinsic fluorescence and fluorescent Ca^{2+} indicators. Our best estimate was obtained using changes in CD ellipticity at 208 and 222 nm as a function of Ca^{2+} concentration. The titration data analyzed with the Hill equation suggest that the apparent K_d of STIM2 EF–SAM is ~0.5 mM at 15 °C, similar to that of STIM1 EF–SAM. This is not surprising given that the amino acid sequence of the Ca^{2+}-binding loop in the EF-hand motif of STIM2 is highly homologous to that of STIM1 (7 out of 12 are identical and 4 similar between the two proteins) (Fig. 1B).

STIM2 EF–SAM is more stable than STIM1 EF–SAM

We employed far-UV CD spectroscopy to probe the secondary structure of STIM1 and STIM2 EF–SAM. The spectrum of Ca^{2+}-loaded STIM2 EF–SAM shows two intense minima at ~208 and 225 nm, indicative of high α-helix content (Fig. 2B). This spectrum is nearly identical to that of STIM1 EF–SAM (Fig. 2A). However, the two homologues behave differently when Ca^{2+} is removed. In the case of Ca^{2+}-free STIM1 EF–SAM (Fig. 2A), the intensity of the 225 nm minimum is much lower compared to the Ca^{2+}-loaded state and a significant blue shift of the 208 nm minimum is observed. These data suggest that apo STIM1 EF–SAM is less well-folded compared with holo as previously interpreted [19]. To our surprise, apo STIM2 EF–SAM does not produce such a large spectral change (Fig. 2B), but rather the spectrum remains nearly identical in shape with a small reduction in intensity for both the 208 and 225 nm minima. These data indicate that under the conditions used, apo STIM2 EF–SAM is appreciably more stable than apo STIM1 EF–SAM, and that STIM2 EF–SAM retains most of its secondary structure even in the absence of Ca^{2+}.

The difference in structural stability between STIM1 and STIM2 was further tested by employing CD temperature melting experiments (Fig. 2C and D). By following the changes in CD ellipticity at 225 nm as a function of temperature, we found that apo STIM2 EF–SAM is significantly more thermally stable than STIM1 EF–SAM (the apparent midpoint of the transition, T_m ~36 °C for STIM2 EF–SAM compared to 21 °C for STIM1 EF–SAM). Similarly, even in the presence of Ca^{2+}, STIM2 EF–SAM has a higher melting temperature than STIM1 EF–SAM (T_m ~50 °C *versus* ~45 °C, respectively). The smaller difference in the thermal stability between Ca^{2+}-loaded and Ca^{2+}-free STIM2 (ΔT_m ~14 °C) compared to that of STIM1 (ΔT_m ~24 °C) is related to the smaller secondary structure change of STIM2 EF–SAM observed upon the removal of Ca^{2+}.

STIM2 EF–SAM shows a Ca^{2+}-dependent conformational change

Although STIM2 EF–SAM does not display a large CD spectral change as observed for STIM1 EF–SAM, the

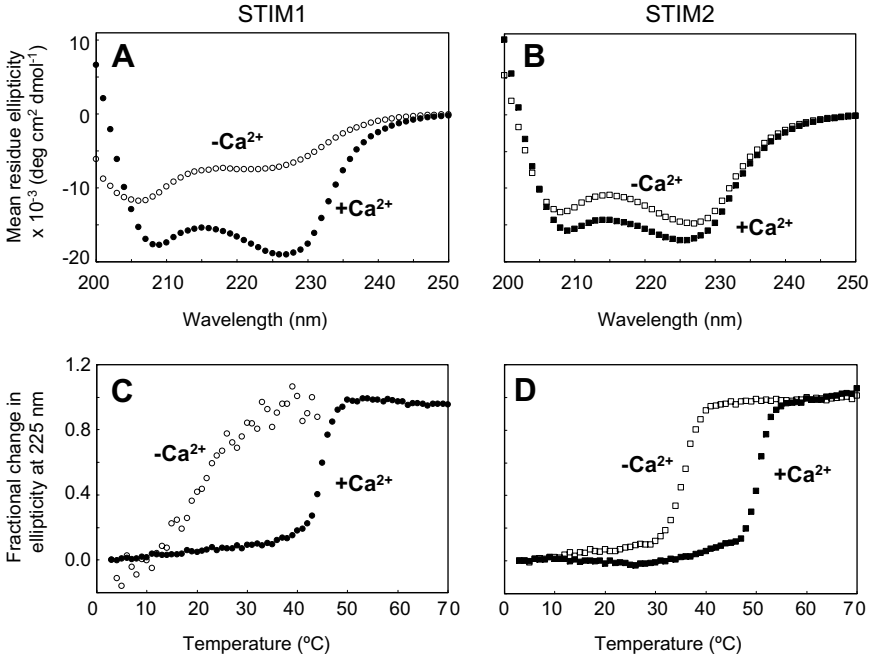

Fig. 2. Ca^{2+}-dependent secondary structure change and thermal stability of EF–SAM. (A) Far-UV CD spectra of apo (○) and holo (●) STIM1 EF–SAM at 4 °C. (B) Far-UV CD spectra of apo (□) and holo (■) STIM2 EF–SAM at 4 °C. (C) Thermal unfolding of apo and holo STIM1 EF–SAM. (D) Thermal unfolding of apo and holo STIM2 EF–SAM. Protein concentrations are from 20 to 40 μM.

increase in negative ellipticity suggests some degree of conformational rearrangement accompanied by Ca^{2+}-binding [20]. In order to further characterize this alteration in the native conformation of STIM2 EF–SAM, we performed NMR experiments. The ^{1}H–^{15}N HSQC spectra of STIM2 EF–SAM in the presence and absence of Ca^{2+} were recorded at 800 MHz (Fig. 3A and B). The well-dispersed peaks indicate that the protein is well-folded in both Ca^{2+}-loaded and Ca^{2+}-free states, consistent with the aforementioned CD studies. More importantly, comparison between the two spectra provides strong evidence for a Ca^{2+}-dependent conformational change. Most notably, the chemical shift of the conserved Gly172 residue in the Ca^{2+}-binding loop of the canonical EF-hand shows a typical behavior of Ca^{2+}-induced conformational responses as documented for numerous EF-hand proteins such as calmodulin [21], troponin C [22], calerythrin [23] and S100 proteins [24] as well as STIM1 EF–SAM [19]. In the Ca^{2+}-loaded state, the most downfield-shifted backbone peak at ~10.3 ppm (^{1}H) and ~112.8 ppm (^{15}N) can be assigned to Gly-172 in STIM2 with a relatively high confidence. This characteristic peak for the Ca^{2+}-loaded state disappears in the Ca^{2+}-free state, presumably being shifted to a crowded spectral region (7.5–8.5 ppm in ^{1}H).

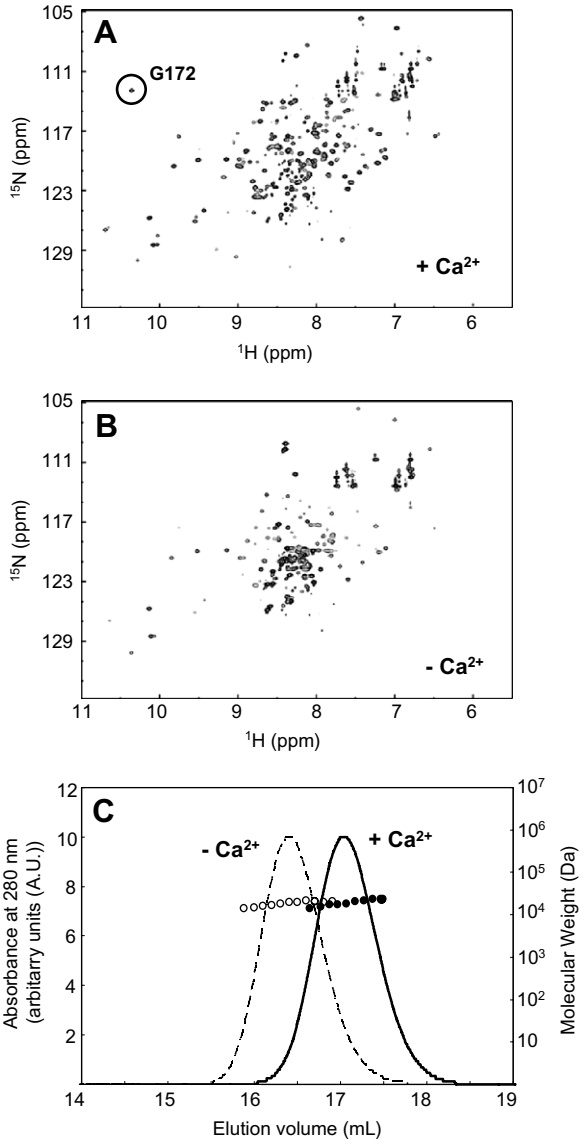

Fig. 3. Ca^{2+}-dependent conformational change of STIM2 EF–SAM. ^{1}H-^{15}N HSQC spectra of Ca^{2+}-loaded (A) and Ca^{2+}-free (B) STIM2 EF–SAM at 4 °C. (C) SEC with in-line MALS in the presence (—) and absence (- - -) of Ca^{2+} at 4 °C. Protein concentrations are at 500 μM.

Unlike STIM1, STIM2 remains monomeric and does not display aggregation by SEC using Superdex HR-200 even in the absence of Ca^{2+} (Fig. 3C). However, a careful inspection of the elution volume reveals that apo STIM2 EF–SAM elutes slightly earlier than the monomeric holo form. The SEC in-line MALS yields a Zimm plot-based molecular mass of 18.6 kDa for the apo state, which is in excellent agreement with that of the holo state (18.3 kDa) as well as the expected mass of STIM2 EF–SAM (17.8 kDa). The size exclusion data together with the MALS data strongly suggest that apo STIM2 EF–SAM is monomeric but less compact (or more extended) in molecular shape than that of holo protein.

Aggregation of apo STIM2 EF–SAM is temperature-dependent

The SEC/MALS data indicate that STIM2 EF–SAM exists as a monomer in both Ca^{2+}-loaded and -depleted forms at 4 °C (Fig. 3C). This is in contrast to what was observed with STIM1 EF–SAM, which forms a dimer and/or oligomer once Ca^{2+} is removed [19]. Considering that EF–SAM of STIM2 is more stable than that of STIM1, we performed NMR and SEC at a higher temperature to examine the relationship between thermal stability and aggregation propensity of STIM2. At 25 °C, the ^{1}H–^{15}N HSQC spectrum of holo STIM2 EF–SAM (data not shown) is very similar to the spectrum recorded at 4 °C (Fig. 3A), with most corresponding peaks showing similar proton and nitrogen chemical shifts. An increase in temperature from 4 to 25 °C dramatically changes the HSQC spectrum of apo STIM2 EF–SAM; unlike the well-dispersed apo spectrum observed at 4 °C (Fig. 3B), the NMR spectrum obtained at 25 °C suffers from severe peak broadening with only a small number of sharp peaks remaining in the 7.5–8.5 ppm (^{1}H) range (Fig. 4A, insert). Interestingly, the spectral changes are similar to those previously observed for apo *versus* holo STIM1 EF–SAM [19]. Consistent with the NMR results, SEC indicates that apo STIM2 EF–SAM undergoes aggregation at 25 °C, as most of the protein elutes in void volume (Fig. 4A).

Apo STIM2 EF–SAM demonstrates a concentration-dependent CD change at high temperature

To further characterize the aggregation propensity of STIM2 EF–SAM, we measured the far-UV CD spectra of apo STIM2 EF–SAM at different protein concentrations

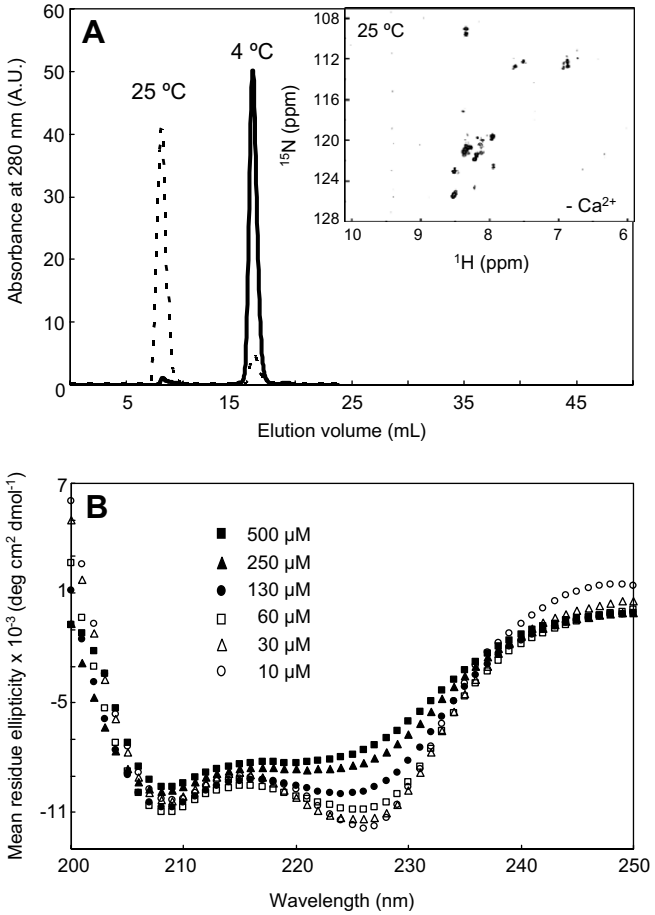

Fig. 4. Temperature-dependent aggregation and concentration-dependent CD change of apo STIM2 EF–SAM. (A) SEC elution profile at 25 °C (- - -) and 4 °C (—). The insert shows ^{1}H–^{15}N HSQC spectrum of apo STIM2 EF–SAM at 25 °C. The protein concentration is at 500 μM. (B) Far-UV CD spectra of apo STIM2 EF–SAM at different concentrations recorded after 70 min incubation at 25 °C.

after 70 min incubation at 25 °C. When the protein concentration is as low as 10 μM, the spectrum is similar to that of apo STIM2 EF–SAM recorded at 4 °C (Fig. 2B). However, when we increased the protein concentration from 30 to 130 μM, the intensity of the negative peak at 225 nm gradually declined. When the protein concentration is increased to 500 μM, the CD spectrum of apo STIM2 EF–SAM shows a single minimum reminiscent of that observed for apo STIM1 EF–SAM. The major differences between STIM1 and STIM2 EF–SAM are in the blue shift and the intensity change at the 208 nm minimum observed for STIM1 EF–SAM, which is less notable for apo STIM2 EF–SAM.

Discussion

In mammalian cells, suppressing STIM1 expression prevents store-operated Ca^{2+} entry and eliminates the Ca^{2+}-depletion dependent activation of CRAC channels [8,9]. Mutations in the EF-hand Ca^{2+}-binding loop disrupt the ability of STIM1 to respond to Ca^{2+}, resulting in constitutively active SOCE even when ER stores are loaded with Ca^{2+} [8,10]. These data provide strong evidence for STIM1 functioning as a Ca^{2+}-dependent activator of SOCE. Although STIM2 contains similar domain architecture and Ca^{2+}-binding sequence as STIM1 (Fig. 1), STIM2 responds to ER Ca^{2+}-depletion differently from STIM1. Suppressing STIM2 expression causes either a modest SOCE inhibition [8] or has little effect [17]; on the other hand, overexpression of STIM2 inhibits SOCE [9,17]. STIM1-mediated SOCE is associated with punctae formation of STIM1 at ER–PM junctions [8,11]. This molecular association on the ER membrane is reversed upon Ca^{2+} restoration in the ER lumen [25].

Our previous study on recombinant STIM1 EF–SAM demonstrated that this N-terminal fragment possesses the ability to bind Ca^{2+} and forms homotypic oligomers and aggregates in the Ca^{2+}-depleted state [19]. In the current study, we carried out comparative biophysical studies on EF–SAM of STIM1 and STIM2 in order to delineate structural characteristics of the Ca^{2+} sensory region, which are specific to each of the homologues. The apparent inability of STIM2 to form visible punctae in cell imaging studies [17] had prompted us to ask whether or not the monomeric propensity of the protein is a result of high Ca^{2+}-binding ability. When the ER store is depleted, a residual amount of Ca^{2+} might still be sufficient to bind to the protein which remains as a monomer. However, our K_d estimate indicates that the Ca^{2+}-binding affinity of the EF–SAM domain of STIM2 is low, similar to that of STIM1.

Subsequently we investigated the possibility that structural stability of EF–SAM may play a role in STIM protein aggregation propensity. STIM2 displays significantly higher melting temperatures than STIM1 in both Ca^{2+}-free and Ca^{2+}-saturated states: T_m ~36 and 50 °C for apo and holo STIM2, respectively; T_m ~21 and 45 °C for apo and holo STIM1, respectively. Most notable is the fact that apo STIM2 EF–SAM is significantly more stable (ΔT_m ~15 °C) compared to apo STIM1 EF–SAM. This observation is in parallel with the SEC data and far-UV CD spectra which show that apo STIM2 EF–SAM possesses high stability as a monomer and retains its high α-helicity. In contrast, apo STIM1 EF–SAM possesses significantly reduced secondary structure and readily aggregates. The tendency of STIM2 EF–SAM to exist as a monomer even in the absence of Ca^{2+} suggests that the increased stability may prevent STIM2 from aggregation.

We further investigated the relationship between structural stability and aggregation propensities using CD spectroscopy. The concentration-dependent CD change of Ca^{2+}-free STIM2 EF–SAM (Fig. 4B) suggests the existence of two conformation states in the absence of Ca^{2+}. At a protein concentration of 10 μM, the far-UV CD spectrum is indicative of a well-folded, highly α-helical protein, similar to the highly structured Ca^{2+}-loaded monomer. A slight decrease in both minima is notable, indicating some

conformational alterations upon Ca^{2+} depletion, which represents a transition to the well-folded monomeric state of apo STIM2. This difference in CD for apo *versus* holo STIM2 is somewhat analogous to what has been observed for calmodulin [26] and other EF-hand proteins [27,28]. At protein concentration of 500 μM, apo STIM2 aggregates and displays a CD spectrum with a markedly reduced 225 nm minimum, which may signify a less α-helical or partially unfolded structure. These observations were made at 25 °C, but similar data were also obtained at 4 °C. At the low temperature, freshly prepared, highly concentrated apo STIM2 EF–SAM exists as a monomer and displays a well-folded CD spectrum. When stored at 4 °C for more than one month, the CD spectrum becomes similar to the one obtained at high concentration and at 25 °C (data not shown). These data strongly suggest the existence of an equilibrium between the two conformation states of apo STIM2 EF–SAM: a well-folded monomeric state and a less α-helical/partially unstructured state which leads to aggregation. The well-structured conformer exists predominantly at lower protein concentrations and lower temperatures whereas the population of the partially unstructured conformer increases and shifts the equilibrium in favor of the detectable aggregates at higher protein concentrations and higher temperatures.

In light of the present data obtained for STIM2 EF–SAM, one can speculate a similar mechanism of aggregation for STIM1. The CD spectrum of apo STIM1 EF–SAM suggests a moderately unfolded protein [29] and the protein is found largely aggregated in the absence of Ca^{2+}. STIM1 EF–SAM may undergo immediate unfolding and aggregation upon Ca^{2+} depletion. The fast kinetics of unfolding and aggregation of STIM1 EF–SAM may hinder the detection of an intermediate apo state, which is presumably monomeric and well-folded as observed for STIM2 EF–SAM. The lower structural stability of STIM1 EF–SAM relative to STIM2 EF–SAM may be responsible for the higher tendency of STIM1 to aggregate *in vitro* and perhaps *in vivo*.

In summary, the present study unveiled remarkable differences in structural stability and aggregation properties between STIM1 and STIM2 EF–SAM domains. The higher stability of apo STIM2 EF–SAM monomer provides an excellent opportunity to elucidate the atomic-resolution structure of the Ca^{2+}-free conformation of STIM molecules by NMR or X-ray crystallography.

Acknowledgments

This paper is dedicated to the memory of Professor Setsuro Ebashi. This work was supported by a Canadian Institutes of Health Research (CIHR) operating grant (to M.I.) and a Natural Sciences and Engineering Research Council of Canada postdoctoral fellowship (to P.B.S.). M.I. is a Canada Research Chair in cancer structural biology.

References

[1] M.J. Berridge, P. Lipp, M.D. Bootman, The versatility and universality of calcium signalling, Nat. Rev. Mol. Cell Biol. 1 (2000) 11–21.
[2] M.J. Berridge, M.D. Bootman, H.L. Roderick, Calcium signalling: dynamics, homeostasis and remodelling, Nat. Rev. Mol. Cell Biol. 4 (2003) 517–529.
[3] M.J. Berridge, The endoplasmic reticulum: a multifunctional signaling organelle, Cell Calcium 32 (2002) 235–249.
[4] A.B. Parekh, R. Penner, Store depletion and calcium influx, Physiol. Rev. 77 (1997) 901–930.
[5] J.W. Putney Jr., L.M. Broad, F.J. Braun, J.P. Lievremont, G.S. Bird, Mechanisms of capacitative calcium entry, J. Cell Sci. 114 (2001) 2223–2229.
[6] K. Venkatachalam, D.B. van Rossum, R.L. Patterson, H.T. Ma, D.L. Gill, The cellular and molecular basis of store-operated calcium entry, Nat. Cell. Biol. 4 (2002) E263–E272.
[7] A.B. Parekh, J.W. Putney Jr., Store-operated calcium channels, Physiol. Rev. 85 (2005) 757–810.
[8] J. Liou, M.L. Kim, W.D. Heo, J.T. Jones, J.W. Myers, J.E. Ferrell Jr., T. Meyer, STIM is a Ca^{2+} sensor essential for Ca^{2+}-store-depletion-triggered Ca^{2+} influx, Curr. Biol. 15 (2005) 1235–1241.
[9] J. Roos, P.J. DiGregorio, A.V. Yeromin, K. Ohlsen, M. Lioudyno, S. Zhang, O. Safrina, J.A. Kozak, S.L. Wagner, M.D. Cahalan, G. Velicelebi, K.A. Stauderman, STIM1, an essential and conserved component of store-operated Ca^{2+} channel function, J. Cell Biol. 169 (2005) 435–445.
[10] M.A. Spassova, J. Soboloff, L.P. He, W. Xu, M.A. Dziadek, D.L. Gill, STIM1 has a plasma membrane role in the activation of store-operated $Ca(^{2+})$ channels, Proc. Natl. Acad. Sci. USA 103 (2006) 4040–4045.
[11] S.L. Zhang, Y. Yu, J. Roos, J.A. Kozak, T.J. Deerinck, M.H. Ellisman, K.A. Stauderman, M.D. Cahalan, STIM1 is a Ca^{2+} sensor that activates CRAC channels and migrates from the Ca^{2+} store to the plasma membrane, Nature 437 (2005) 902–905.
[12] M.M. Wu, J. Buchanan, R.M. Luik, R.S. Lewis, Ca^{2+} store depletion causes STIM1 to accumulate in ER regions closely associated with the plasma membrane, J. Cell Biol. 174 (2006) 803–813.
[13] X. Cai, Molecular evolution and functional divergence of the Ca^{2+} sensor protein in store-operated Ca^{2+} entry: stromal interaction molecule, PLoS ONE 2 (2007) e609.
[14] R.T. Williams, S.S. Manji, N.J. Parker, M.S. Hancock, L. Van Stekelenburg, J.P. Eid, P.V. Senior, J.S. Kazenwadel, T. Shandala, R. Saint, P.J. Smith, M.A. Dziadek, Identification and characterization of the STIM (stromal interaction molecule) gene family: coding for a novel class of transmembrane proteins, Biochem. J. 357 (2001) 673–685.
[15] R.T. Williams, P.V. Senior, L. Van Stekelenburg, J.E. Layton, P.J. Smith, M.A. Dziadek, Stromal interaction molecule 1 (STIM1), a transmembrane protein with growth suppressor activity, contains an extracellular SAM domain modified by N-linked glycosylation, Biochim. Biophys. Acta 1596 (2002) 131–137.
[16] S.S. Manji, N.J. Parker, R.T. Williams, L. van Stekelenburg, R.B. Pearson, M. Dziadek, P.J. Smith, STIM1: a novel phosphoprotein located at the cell surface, Biochim. Biophys. Acta 1481 (2000) 147–155.
[17] J. Soboloff, M.A. Spassova, T. Hewavitharana, L.P. He, W. Xu, L.S. Johnstone, M.A. Dziadek, D.L. Gill, STIM2 is an inhibitor of STIM1-mediated store-operated Ca2+ Entry, Curr. Biol. 16 (2006) 1465–1470.
[18] J. Soboloff, M.A. Spassova, X.D. Tang, T. Hewavitharana, W. Xu, D.L. Gill, Orai1 and STIM reconstitute store-operated calcium channel function, J. Biol. Chem. 281 (2006) 20661–20665.
[19] P.B. Stathopulos, G.Y. Li, M.J. Plevin, J.B. Ames, M. Ikura, Stored Ca^{2+} depletion-induced oligomerization of stromal interaction molecule 1 (STIM1) via the EF–SAM region: An initiation mechanism for capacitive Ca^{2+} entry, J. Biol. Chem. 281 (2006) 35855–35862.

[20] S.M. Gagne, S. Tsuda, M.X. Li, M. Chandra, L.B. Smillie, B.D. Sykes, Quantification of the calcium-induced secondary structural changes in the regulatory domain of troponin-C, Protein Sci. 3 (1994) 1961–1974.

[21] M. Zhang, T. Tanaka, M. Ikura, Calcium-induced conformational transition revealed by the solution structure of apo calmodulin, Nat. Struct. Biol. 2 (1995) 758–767.

[22] L. Spyracopoulos, M.X. Li, S.K. Sia, S.M. Gagne, M. Chandra, R.J. Solaro, B.D. Sykes, Calcium-induced structural transition in the regulatory domain of human cardiac troponin C, Biochemistry 36 (1997) 12138–12146.

[23] H. Aitio, A. Annila, S. Heikkinen, E. Thulin, T. Drakenberg, I. Kilpelainen, NMR assignments, secondary structure, and global fold of calerythrin, an EF-hand calcium-binding protein from *Saccharopolyspora erythraea*, Protein Sci. 8 (1999) 2580–2588.

[24] A.C. Drohat, D.M. Baldisseri, R.R. Rustandi, D.J. Weber, Solution structure of calcium-bound rat S100B(betabeta) as determined by nuclear magnetic resonance spectroscopy, Biochemistry 37 (1998) 2729–2740.

[25] J. Liou, M. Fivaz, T. Inoue, T. Meyer, Live-cell imaging reveals sequential oligomerization and local plasma membrane targeting of stromal interaction molecule 1 after Ca^{2+} store depletion, Proc. Natl. Acad. Sci. USA 104 (2007) 9301–9306.

[26] S.R. Martin, P.M. Bayley, The effects of Ca^{2+} and Cd^{2+} on the secondary and tertiary structure of bovine testis calmodulin. A circular-dichroism study, Biochem. J. 238 (1986) 485–490.

[27] R.E. Hughes, P.S. Brzovic, A.M. Dizhoor, R.E. Klevit, J.B. Hurley, Ca^{2+}dependent conformational changes in bovine GCAP-2, Protein Sci. 7 (1998) 2675–2680.

[28] M.N. Alexis, W.B. Gratzer, Interaction of skeletal myosin light chains with calcium ions, Biochemistry 17 (1978) 2319–2325.

[29] N. Greenfield, G.D. Fasman, Computed circular dichroism spectra for the evaluation of protein conformation, Biochemistry 8 (1969) 4108–4116.

[30] S. Parvez, A. Beck, C. Peinelt, J. Soboloff, A. Lis, M. Monteilh-Zoller, D.L. Gill, A. Fleig, R. Penner, STIM2 protein mediates distinct store-dependent and store-independent modes of CRAC channel activation, Faseb J. (2007).